DE GRUYTER OPEN

PbS nanopowder – synthesis, characterization and antimicrobial activity

M. SUGANYA, A.R. BALU*

PG and Research Department of Physics, AVVM Sri Pushpam College, Poondi-613 503, Tamilnadu, India

Lead sulphide (PbS) nanopowder was synthesized by a simple soft chemical route using lead nitrate and thiourea as precursor salts. The as-synthesized nanopowder was characterized by XRD, SEM, EDX, FT-IR, PL, Raman and magnetic measurements. XRD studies reveal the polycrystalline nature of the powder. The powder exhibits face-centered cubic structure with a strong (2 0 0) preferential orientation. The presence of Pb and S in the powder is confirmed by energy dispersive X-ray analysis. The peaks observed at 1112 cm^{-1} and at 606 cm^{-1} in the FT-IR spectrum are related to heteropolar diatomic molecules of PbS. The Raman peak shift at 173 cm^{-1} might have originated from the combination of longitudinal and transverse acoustic phonon modes associated with PbS crystal. The M-H loop confirms the paramagnetic nature of the as-synthesized PbS nanopowder. The nanopowder has significant antimicrobial activity against certain bacteria and fungi strains which make it suitable as antimicrobial agent against pathogenic microorganisms.

Keywords: *X-ray diffraction; photoluminescence; energy dispersive X-ray analysis; antimicrobial properties*

1. Introduction

Nanostructured semiconducting chalcogenide materials have gained considerable attention over their bulk counterparts due to their non-linear, luminescence and useful physical and chemical properties [1]. Among the semiconducting chalcogenide nanomaterials, lead sulphide (PbS) possesses specific optical and electronic properties due to the quantum size and dielectric confinement effects which make it more suitable in light emitting diodes, infrared detectors, optical fibers, infrared lasers, solar energy panels, etc. [2–4]. Because of tuneable nature of first excitonic transition from the visible to the infrared, PbS nanomaterials are well suited for infrared related applications [5]. PbS is an important direct band gap material with a band gap of 0.41 eV, large exciton Bohr radius of 18 nm, high dielectric constant of 18 and high carrier mobility of 0.44 $cm^2 \cdot V^{-1} \cdot s^{-1}$ [6, 7]. Due to these properties, PbS possesses third order non-linear optical response 30 times better than that of GaAs and 1000 times better than CdS

nanoparticles of similar size. Besides, PbS has excellent photoconductive properties [8]. In recent years, the emerging infectious diseases and the development of drug resistance against pathogenic bacteria and fungi is a matter of serious concern. Therefore, it is essential to discover new antimicrobial agents from natural and inorganic substances. The advances in the field of nanoscience and nanotechnology provided a gateway to synthesizing organic and inorganic metal particles in nanoscale regime which find applications in water treatment, medicine and therapeutics, synthetic textiles, food processing and packaging products [9]. PbS is a heavy metal based semiconductor which, when synthesized in nanoscale regime, might possess improved chemical, electrical, optical and magnetic properties compared to that of its bulk counterparts, which makes it an efficient antimicrobial agent also. To find the enhancement in the properties of PbS and its suitability as an antimicrobial agent, in this work, PbS nanopowder was synthesized by a simple soft chemical route and the as-synthesized powder was characterized by various techniques, such as XRD, SEM, EDX, FT-IR, PL and Raman, respectively. The antimicrobial activity study

---

*E-mail: arbalu757@gmail.com

of the PbS nanopowders was performed by well diffusion method. The simple soft chemical route has been adopted here to synthesize PbS nanopowder as it has many advantages such as high potential, energy saving, etc.

2. Experimental

PbS nanopowder was synthesized by a simple soft chemical route. Lead nitrate, (Pb(NO$_3$)$_2$ and thiourea (SC(NH$_2$)$_2$, of 0.2 M each were used as precursor salts. The salts were dissolved in deionized water (70 mL in volume) and the pH value of this solution was found to be equal to 7.4. To this solution, 10 mL of liquid ammonia was added and the pH value was made equal to 12. The resultant solution was stirred continuously for 6 h and care was taken to maintain the pH value of the solution constant at 12 by adding few drops of liquid ammonia. After stirring, the solution was kept undisturbed for 12 hours and the final product was washed, filtered and then calcined at 150 °C for 2 h. The obtained product was smashed in a mortar and again it was subjected to heat treatment at 100 °C for 30 min to get black colored PbS nanopowder. The crystal structure of the powder was analyzed using X-ray diffractometer (PANalytical-PW 340/60 X'Pert PRO). The surface morphology and the elemental composition of the powder were investigated using scanning electron microscope (HITACHI S-3000H) and energy dispersive X-ray analysis. The Fourier transform infrared (FT-IR) spectra were recorded using PerkinElmer RX-1 FT-IR spectrophotometer. PL and Raman studies were performed with a Varian Cary Eclipse Fluorescence Spectrophotometer and Renishaw Invia Laser Raman microscope using a 18 mW 633 nm He–Ne laser. The magnetic properties of the PbS nanopowder were studied using vibrating sample magnetometer (Lakeshore VSM 7410). The antimicrobial activity studies were performed by agar well diffusion method against three bacterial (*Bacterium staphylococcus aureus*, *Escherichia coli* and *Bacillus cereus*) and two fungi (*Aspergillus niger* and *Aspergillus terrus*) strains.

3. Results and discussion

3.1. Structural determination

The XRD pattern of PbS nanopowder synthesized by soft chemical method, shown in Fig. 1, confirmed its polycrystalline nature.
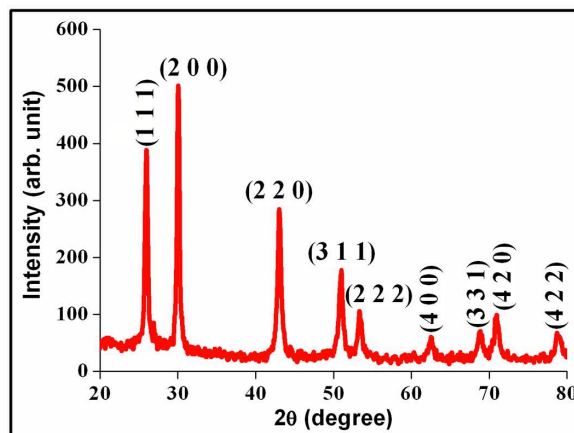
Fig. 1. XRD pattern of PbS nanopowder synthesized by a simple soft chemical route.

The diffraction peaks observed at 2θ values approximately equal to 25.93°, 30.06°, 43.02°, 50.99°, 53.41°, 62.52°, 68.85° and 70.93° indexed to (1 1 1), (2 0 0), (2 2 0), (3 1 1), (2 2 2), (4 0 0), (3 3 1) and (4 2 0) planes fit well with face centered cubic structure of galena PbS (JCPDS Card No. 65-2935). It can be observed from the XRD pattern that the as-synthesized PbS powder exhibits a (2 0 0) preferential orientation. The preferential orientation along the (2 0 0) plane observed here exactly matches with the results reported by Rajashree et al. [3] for undoped and doped PbS thin films. From the XRD pattern, the microstructural parameters such as the lattice parameter (a), crystallite size (D), strain (ϵ) and dislocation density (δ) were calculated for the (2 0 0) plane using the formulae [10, 11]:

$$\frac{1}{d^2} = \frac{h^2 + k^2 + l^2}{a^2} \qquad (1)$$

$$D = \frac{0.9\lambda}{\beta \cos\theta} \qquad (2)$$

$$\varepsilon = \frac{\beta \cos \theta}{4} \qquad (3)$$

$$\delta = \frac{1}{D^2} \, lines/m^2 \qquad (4)$$

The lattice parameter, crystallite size, strain and dislocation density values were found to be equal to 5.946 Å, 27.88 nm, 1.243 × 10^{-3} and 1.287 × 10^{15} lines/m², respectively.

3.2. Surface morphology and elemental analysis

Fig. 2a shows the SEM image of PbS nanopowder. It can be seen that the surface seems to be very smooth, composed of tightly packed grains.
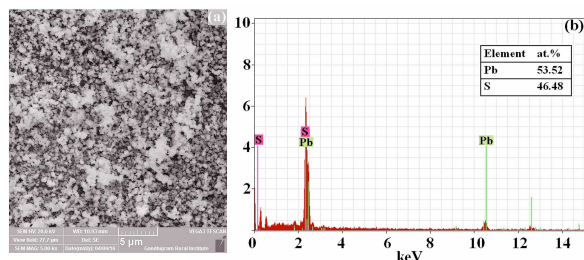
Fig. 2. (a) SEM image and (b) EDX spectrum of PbS nanopowder.

Star shaped grains corresponding to PbS nanopowder were also observed throughout the entire surface. The EDX spectrum (Fig. 2b) confirms the presence of Pb and S in the nanopowder. The atomic percentage composition of the elements Pb and S is given in the inset table of Fig. 2b. It is observed that the as-synthesized nanopowder was found to be deficient with sulfur which plays a vital role in improving its antifungi activity (Section 3.7).

3.3. FT-IR analysis

The Fourier-Transform Infrared (FT-IR) spectrum of PbS nanopowder is shown in Fig. 3.

The peak at 1946 cm^{-1} corresponds to C=O stretching vibrations related to carbonyl group. The weak band observed at 1628 cm^{-1} is attributed to the bending vibration modes of water
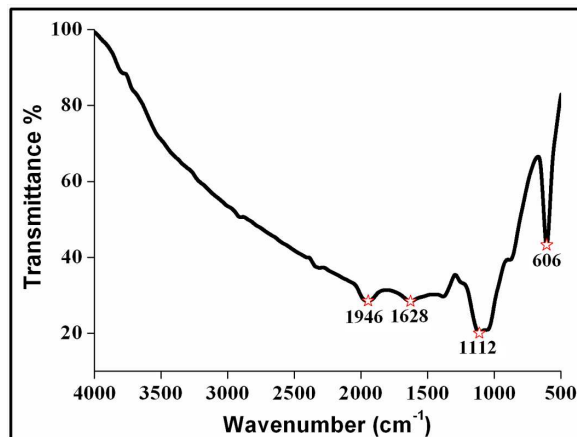
Fig. 3. FT-IR spectrum of the PbS nanopowder.

(H–O–H) [12], which might be due to the aqueous medium used to synthesize the PbS nanopowder. The peaks at 1112 cm^{-1} and 606 cm^{-1} are due to heteropolar diatomic molecules of lead sulphide [13]. Besides, no strong bands associated with Pb–S stretching and bending vibrations are observed in the FT-IR spectrum as the bond associated with Pb–S is mainly electrovalent in nature [14]. Force constant k has been calculated using the equation [15]:

$$k = 4\pi^2 \left(\bar{\omega}^2 \right) c^2 \mu \qquad (5)$$

where $\bar{\omega}$ is the vibrational frequency and wavenumber, c is the velocity of light and μ is the reduced mass of the system. The force constant for PbS is found to be equal to 660 N·m^{-1}.

3.4. PL studies

Fig. 4 shows the room temperature PL spectrum of PbS nanopowder synthesized by simple soft chemical method, excited at wavelength λ = 400 nm.

Emission peaks are observed at 408 nm, 421 nm, 487 nm and 520 nm, respectively. The sharp ultraviolet peak observed at 408 nm (3.04 eV) infers that the synthesized PbS nanopowder has less crystal defects. This peak may be attributed to the direct transition to the valence band from the conduction band. The peak at 421 nm (2.95 eV) might be due to an exciton bound to a donor level [16]. The small intensity peak
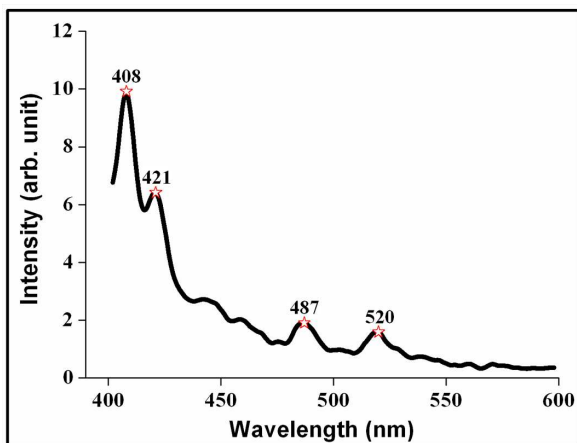
Fig. 4. PL spectrum of the PbS nanopowder.

observed at 487 nm (2.55 eV) corresponds to band-edge luminescence [17]. The green emission peak observed at 520 nm (2.39 eV) could be related to excitonic transitions, which might be due to the presence of electron-hole recombination via trap state or imperfection site [18].

3.5. Raman studies

The Raman spectra of PbS nanopowder are shown in Fig. 5.
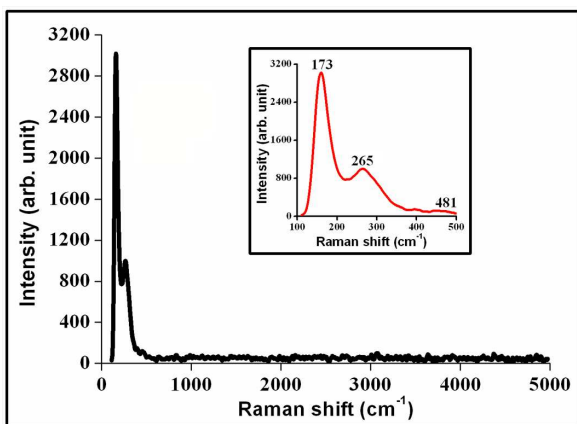
Fig. 5. Raman spectrum of the PbS nanopowder.

The magnified part of the spectrum in the region of 100 cm^{-1} to 500 cm^{-1} is displayed in the inset of Fig. 5. From the inset, it is observed that the spectrum shows emission peaks at 173 cm^{-1}, 265 cm^{-1} and 481 cm^{-1}. The band centered at

173 cm^{-1} might have originated from the combination of longitudinal and transverse acoustic phonon modes associated with PbS crystal [19]. The peak at 265 cm^{-1} may be related to PbO formation due to photodegradation of PbS [20]. The peak at 481 cm^{-1} might be caused by formation of PbO$_2$ as a result of laser photooxidation product of PbS [21]. Ovsyannikov et al. [22] observed a similar peak at 510 cm^{-1} assigned to the formation of PbO$_2$. This peak came from the second overtone of fundamental longitudinal optical (LO) phonon mode 3 LO [23].

3.6. Magnetic properties

Vibrating sample magnetometer (Lakeshore VSM 7410) was used to investigate the magnetic properties of as-synthesized PbS nanopowder at room temperature. Fig. 6 shows the M-H loop of the PbS nanopowder.
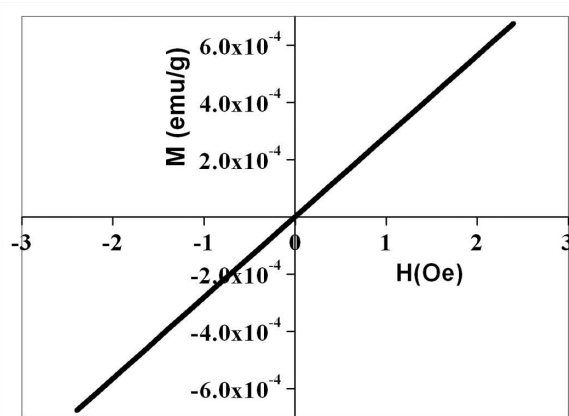
Fig. 6. M-H loop of the PbS nanopowder.

It is observed that the curve passes through zero which confirms the paramagnetic nature of the as-synthesized nanopowder. No signs of ferromagnetic and anti-ferromagnetic interactions were observed in the nanopowder.

3.7. Antimicrobial activity

Antimicrobial activity involves relation between compounds that locally kill bacteria/fungi or slow down their growth without being in general toxic to the surrounding tissue. The most commonly used antimicrobial agents can be classified

as either bacterial, which kill bacteria, or bacteriostatic which slow down bacterial growth. However, with their broad use and abuse, the emergence of bacterial resistance to antibacterial drugs has become a common phenomenon, which is a major problem. Because of the fact that the bacteria/fungi develop resistance against many common antimicrobial agents, infectious diseases continue to be one of the greatest health challenges worldwide. Also adequate usage of these antimicrobial agents produces adverse side effects besides resisting the pathogenic microorganisms. This prompted the development of alternative strategies to treat bacteria and fungi diseases. One such strategy is to identify new nanoscale materials which can emerge as novel antimicrobial agents. These nanoscale materials, due to their high surface area to volume ratio, have improved mechanical, chemical, electrical, optical, magnetic properties compared to that of their bulk counterparts, which makes them act as more efficient antimicrobial agents.

To assess the suitability of the PbS nanopowder as an antimicrobial agent, the following bacteria (*Staphylococcus aureus*, *Escherichia coli*, *Bacillus cereus*) and fungi (*Aspergillus niger*, *Aspergillus terrus*) strains were tested by agar well diffusion method. The stock cultures of bacteria and fungi were maintained on nutrient agar and potato dextrose slants at 4 °C. Inoculums was prepared by suspending a loop full of bacteria and fungi cultures into 10 mL of nutrient broth inoculated at 37 °C (±2 °C) for 24 h to 48 h. Nutrient agar plates were swabbed with cultures of the above mentioned bacteria and fungi and 5 mm diameter wells were bored on the agar plates using sterile cork borer. PbS nanopowders with different concentrations 0.01 g and 0.02 g were put into the wells, and the plates were left for 1 h to allow pre-incubation diffusion in order to minimize the effects of variation in time between the application of different solutions. The plates were incubated in an upright position maintained at 37 °C for 24 hours.

Fig. 7 shows the antimicrobial activity of the PbS nanopowders against the bacteria and fungi strains, which is confirmed by the formation of zones around the powders.
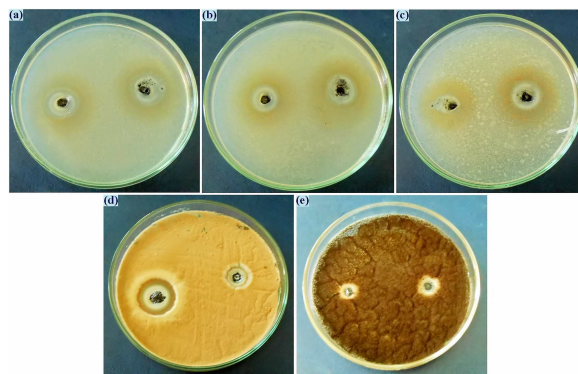
Fig. 7. Antimicrobical activity of PbS nanopowders against bacteria (a) *Staphylococcus aureus*, (b) *Escherichia coli*, (c) *Bacillus cereus* and fungi (d) *Aspergillus niger*, (e) *Aspergillus terrus* strains.

The antimicrobial activity of the PbS nanopowders was estimated by measuring the diameters of zone of inhibition in millimetre scale. The samples were tested in triplicates and the average values of the diameters of zone of inhibition obtained are given in Table 1.

Significant antimicrobial activity of the nanopowders was observed against gram-negative bacteria (*E. coli*), gram-positive bacteria (*B. cereus*) and against fungi (*A. terreus*). The nanopowders show moderate antimicrobial activity against gram-positive bacteria (*S. aureus*) and fungi (*A. niger*). The significant antibacterial activity possessed by PbS nanopowders against gram-negative bacteria, when compared to that of the gram-positive bacteria, might be due to the cell wall nature of the bacteria. The gram-negative bacteria possess slender layer of membrane, whereas the gram-positive bacteria possess deep layer of membrane, consisting of linear polysaccharide chains. The antibacterial activity of PbS nanopowders is ascribed to a combination of factors that include generation of reactive oxygen species (ROS) and efflux mechanisms leading to the release of constituent ions [24]. It has been reported earlier that Pb^{2+} ions cause toxicity by interacting with nucleic acids by binding to essential respiratory proteins through oxidative damage caused by production of reactive oxygen

Table 1. Zone of inhibition of PbS nanopowders against certain bacteria and fungi strains.

Microorganism		Zone of inhibition [mm] PbS powder concentration	
		0.01 g	0.02 g
Bacteria	*Escherichia coli* (*E. coli*)	12	14
	Staphylococcus aureus (*S. aureus*)	5	10
	Bacillus cereus (*B. cereus*)	7	11
Fungi	*Aspergillus terrus* (*A. Terreus*)	6	19
	Aspergillus niger (*A. niger*)	4	6

species [25]. Pb^{2+} ions enter bacterial cells via transport systems and the cells respond to it by metal inducible resistance mechanisms.

The presence of intrinsic defects in PbS nanopowder produces electron-hole pairs, as evidenced by the PL and Raman spectra. These holes react with water, producing H^+ and OH^- ions and the electrons convert the dissolved oxygen molecules to superoxide radical anions. So obtained superoxide radical anions react with H^+ producing HO_2 radicals which then get converted to hydrogen peroxide anions (HO_2^-). Hydrogen peroxide is then obtained by the reaction of these anions with hydrogen ions, and the obtained hydrogen peroxide penetrates the fungi cell membrane and disrupts it due to oxidative stress [26]. In PbS nanopowder, the presence of S vacancies is the most obvious source of band transitions leading to the generation of H_2O_2. The presence of S vacancies has been well acknowledged by the EDX analysis (Section 3.2). The observations made here confirm that the PbS nanopowder emerges as a potential antibacterial and antifungal agent thereby resisting the growth of pathogenic bacteria which cause respiratory illness, pneumonia, urinary infections, food borne illness and fungi related infections.

4. Conclusions

PbS nanopowder was successfully synthesized by a simple soft chemical route method. XRD studies confirmed that the PbS nanopowder exhibited face-centered cubic structure with a preferential orientation along the (2 0 0) plane. The lattice parameter, crystallite size, strain and dislocation density values were found to be equal to 5.946 Å, 27.88 nm, 1.243×10^{-3} and 1.287×10^{15} lines/m^2, respectively. The FT-IR spectra confirmed the presence of stretching vibrations of Pb–S at 606 cm^{-1}. The PbS nanopowder was found to be paramagnetic in nature. The antimicrobical activities of PbS nanopowders confirmed that they can be used as an antimicrobial agent resisting the growth of pathogenic bacteria and fungi strains which make them suitable for nanodrug design as well as medicinal and pharmaceutical applications.

References

[1] BAGADE C.S., GHANWAT V.B., KNOT K.V., BHOS-ALE P.N., *Mater. Lett.*, 164 (2016), 52.
[2] VOIT J., *Rep. Prog. Phys.*, 58 (1994), 977.
[3] RAJASHREE C., BALU A.R., NAGARETHINAM V.S., *Surf. Eng.*, 31 (2015), 316.
[4] PETERSON J.J., KRAUSS T.D., *Nano Lett.*, 6 (2006), 510.
[5] MCDONALD S.A., KONSTANTATOS G., ZHANG S., CYR P.W., KLEM J.D.E., LEVINA L., SARGENT E.H., *Nat. Mater.*, 4 (2005), 138.
[6] INUK K., FRANK W.W., *J. Opt. Soc. Am.*, 14 (1997), 1632.
[7] SCANLON W.W., *Phys. Rev.*, 109 (1958), 47.
[8] WANG Y., *Accounts Chem. Res.*, 24 (1991), 133.
[9] GAJJAR P., PETTEE B., BRITT D.W., HUANG W., JOHSNON W.P., ANDERSON J., *J. Biol. Eng.*, 3 (2009), 9.
[10] USHARANI K., BALU A.R., *Acta Metall. Sin.*, 28 (2015), 64.
[11] RAVISHANKAR S., BALU A.R., ANBARASI M., NAGARETHINAM V.S., *Optik*, 126 (2015), 2550.

[12] VAEZI M.R., SADRNEZHAAD S.K., *Mater. Design*, 28 (2007), 515.

[13] BORHADE A.V., UPHADE B.K., *Chalcogenide Lett.,* 9 (2012), 299.

[14] PAWAR S.B., SHAIKH J.S., DEVAN R.S., MA Y.R., HARANATH D., BHOSALE P.N., PATIL P.S., *Appl. Surf. Sci.*, 258 (2011), 1869.

[15] BANWELL C.N., MCCASH E.M., *Fundamentals of molecular spectroscopy*, Tata McGraw Hill, New Delhi, 2010.

[16] SELVAN G., ABUBAKER M.P., USHARANI K., BALU A.R., *Surf. Eng.*, 32 (2015), 212.

[17] MURALI G., REDDY D.A., SAMBASAIVAM S., GIRIBABU G., VIJAYALAKSHMI R.P., VENUGOPAL R., REDDY B.K., *Mater. Lett.*, 93 (2013), 149.

[18] CHAURE S., CHAURE N.B., PANDEY R.K., *Physica E*, 28 (2005), 436.

[19] SMITH G.D., FIRTH S., CLARK R.J.H., CARDONA M., *J. Appl. Phys.*, 92 (2002), 4375.

[20] SHAPTER J.G., BROOKER M.H., SKINNER W.M., *Int. J. Miner. Process.*, 60 (2000), 199.

[21] BURGIO L., CLARK R.J.H., FIRTH S., *Analyst*, 126 (2001), 222.

[22] OVSYANNIKOV S.V., SHCHENNIKOV V.V., CANTARERO A., CROSS A., TITOV A.N., *Mat. Sci. Eng. A-Struct.*, 462 (2007), 422.

[23] HUANG Q.L., CHEN H., WU C.L., ZHANG Y.C., *Mater. Lett.*, 64 (2010), 1891.

[24] PERKAS N., LIPOVSKY A., AMIRIAN G., NITZAN Y., GEDANKEN A., *J. Mater. Chem.*, 8 (2013), 5309.

[25] STOHS S.J., BAGEHI D., *Free Radical Bio. Med.*, 18 (1995), 321.

[26] APPLEROT G., LIPOVSKY A., DROR R., PERKAS N., NITZAN Y., LUBART R., GEDANKEN A., *Adv. Funct. Mater.*, 19 (2009), 842.